Immunity, Vol. 15, 691–701, November, 2001, Copyright ©2001 by Cell Press

Exclusion of CD43 from the Immunological Synapse Is Mediated by Phosphorylation-Regulated Relocation of the Cytoskeletal Adaptor Moesin

Jérôme Delon,[1] Kozo Kaibuchi,[2] and Ronald N. Germain[1,3]
[1] Laboratory of Immunology
Lymphocyte Biology Section
National Institute of Allergy and Infectious Diseases
National Institutes of Health
Bethesda, Maryland 20892
[2] Department of Cell Pharmacology
Nagoya University Graduate School of Medicine
Aichi 466-8550
Japan

Summary

Formation of the immunological synapse requires TCR signal-dependent protein redistribution. However, the specific molecular mechanisms controlling protein relocation are not well defined. Moesin is a widely expressed phospho-protein that links many transmembrane molecules to the cortical actin cytoskeleton. Here, we demonstrate that TCR-induced exclusion of the large sialoprotein CD43 from the synapse is an active event mediated by its reversible binding to moesin. Our results also reveal that relocalization of moesin is associated with changes in the phosphorylation status of this cytoskeletal adaptor protein. Finally, these findings raise the possibility that the change in moesin localization resulting from TCR engagement modifies the overall topology of the lymphocyte membrane and facilitates molecular interactions at the site of presenting cell contact.

Introduction

Activation of T lymphocytes is initiated by interaction of clonally distributed antigen receptors (TCR) with membrane-associated peptide-MHC ligands on antigen-presenting cells (APC). Signaling resulting from these recognition events begins within seconds and persists for hours, accompanied by additional inputs from other receptor/counter-receptor interactions that are concentrated in the zone of T cell-APC contact. Because this resembles the information transfer at specialized junctions between neurons or between nerves and muscles, this region of interaction between the lymphocyte and the APC is referred to as the "immunological synapse" (Acuto and Cantrell, 2000; Delon and Germain, 2000; Lanzavecchia and Sallusto, 2000; van der Merwe et al., 2000; Bromley et al., 2001).

It has been known for a number of years that signaling at the synapse leads to reorientation of the microtubule-organizing center of the lymphocyte toward the zone of contact with the APC, accompanied by the polarization of protein secretion to this region of the cell (Kupfer et al., 1987; Poo et al., 1988). However, only recently has the existence of a spatially complex distribution of membrane proteins and submembrane molecules within the synaptic region been appreciated (Monks et al., 1998). High-resolution microscopy using both fixed and living cells has revealed a concentric ring pattern of protein distribution within a few minutes of T cell contact with an APC bearing stimulatory peptide/MHC ligands (van der Merwe et al., 2000). TCRs are concentrated in a small zone in the center of the contact region at 2–3 times their density elsewhere on the cell membrane. A ring of the integrin LFA-1 surrounds this central zone. Under the membrane, the localization of the cytoskeletal adaptor protein talin mirrors the LFA-1 distribution, whereas beneath the central accumulation of TCRs, nearly the entire cellular pool of PKC-θ can be found (Monks et al., 1997, 1998; Grakoui et al., 1999).

Early models seeking to explain this patterning were based on the notion that protein size played a key role (Davis and van der Merwe, 1996; Shaw and Dustin, 1997). The localization of shorter molecules such as the accessory molecule CD2 near the TCR and of taller molecules like LFA-1 further from the center of the contact zone is in general accord with this hypothesis (Dustin et al., 1998; Monks et al., 1998; Grakoui et al., 1999; Leupin et al., 2000; van der Merwe et al., 2000). These proposals implied a relatively passive origin for protein distribution in the synapse, based on forces between membranes that "squeezed" larger molecules out from the area of close membrane contact and into a peripheral position. A more recent mathematical model has more specifically ascribed the spatiotemporal development of the immunological synapse to a combination of receptor-ligand affinities and the effect of forces generated by membrane bending due to differences in molecular dimensions of these intercellular protein contacts (Qi et al., 2001).

Other data raise questions about these "passive" models of synaptic organization, however. For example, CD45, a much larger protein than the TCR, is initially depleted in the central zone, but then reenters this region (Johnson et al., 2000). CD4, which must extend further from the T cell membrane than the TCR to contact the membrane-proximal regions of MHC molecules on the APC, is first colocalized with the TCR in the central region and then excluded (Krummel et al., 2000). Most importantly, drug treatments or genetic manipulations that interfere with the function of the cytoskeleton prevent T-APC conjugate formation and organized synapse development, indicating a role for active rather than passive movement of molecules in establishing the polarized distribution of proteins in this region of the lymphocyte membrane (Delon et al., 1998a; Wülfing and Davis, 1998; Dustin and Cooper, 2000). Such evidence for active cytoskeletal control of molecular organization within the forming synapse implies that specific, active mechanisms control protein positioning upon T cell-APC contact. In addition, the existence of a large region of relatively flat membrane contact at the synapse as revealed by electron microscopic studies (Delon et al., 1998b) and the requirement for a zone conducive to effective secretion into the synaptic cleft (Kupfer et al.,

[3] Correspondence: ronald_germain@nih.gov

1987) together suggest the occurrence of additional membrane-remodeling events in this region of the cell.

ERM (Ezrin/Radixin/Moesin) proteins are good candidates for participants in the processes that control both membrane molecule distribution and membrane topology during synapse formation. These proteins belong to the Band 4.1 superfamily and are a set of closely related cytoplasmic proteins that act as a bridge between a subset of transmembrane molecules and the subjacent cortical actin cytoskeleton (Mangeat et al., 1999; Tsukita and Yonemura, 1999; Bretscher et al., 2000). These interactions, which can involve molecules such as CD44, CD43, ICAMs, and Fas, depending on the cell type (Tsukita et al., 1994; Helander et al., 1996; Serrador et al., 1997, 1998; Heiska et al., 1998; Yonemura et al., 1998; Parlato et al., 2000), help define cell shape. As shown in many different cell types, the crosslinking function of ERM proteins involves binding through the cytoplasmic domain of integral membrane proteins and is regulated by reversible threonine phosphorylation in the C terminus of the ERM molecules (Simons et al., 1998; Yonemura and Tsukita, 1999).

Although ERM proteins have been extensively studied in other tissues and cell types, their importance in cells of the immune system is largely unknown, although some insights are emerging from recent studies. Sanchez-Madrid's group has reported their presence in the uropod of T cells activated by chemokines (Serrador et al., 1997, 1998; del Pozo et al., 1999). Moesin, which is the dominant member of the ERM family expressed in T lymphocytes (Shcherbina et al., 1999), has also been shown to play a major role in controlling the topology of the T lymphocyte membrane, especially microvillus formation (Takeuchi et al., 1994). However, its subcellular localization following antigen recognition as well as its possible regulation by TCR-specific signals are unknown.

Here we report the results of studies on the TCR-regulated redistribution of moesin during synapse formation. Our data support a model in which antigen-induced exclusion of moesin is responsible for maintaining CD43 outside of the maturing synapse. We propose that the mechanism first involves disanchoring of CD43 from moesin and of the latter from the cortical actin cytoskeleton through moesin dephosphorylation, migration of CD43 away from the middle of the T-APC contact, followed by the reestablishment of these associations through moesin rephosphorylation in a zone excluded from the central core of the synapse. Further exclusion of CD43 to beyond the integrin contact zone depends on this reanchoring event. This "thaw-freeze" model has several implications for possible topologic reorganization of the lymphocyte membrane that facilitates both early surface and later secretory events at the immunological synapse.

Results

Moesin Is Specifically Excluded from the Immunological Synapse

Although synapse formation clearly involves cytoskeletal function, only talin, a member of the Band 4.1 family of proteins, has been extensively studied for its positioning in T cells interacting with antigen-bearing presenting cells. Because it has been reported to be associated with several relevant surface proteins of T cells, we therefore examined the subcellular localization of the cytoskeletal adaptor moesin in 5C.C7 TCR transgenic T cells with fully mature synapses formed after 30 min of interaction with antigen-pulsed LK35.2 B lymphoma cells. Strikingly, moesin molecules were excluded from the region of T-APC contact (Figure 1A), as seen in both cross-sectional (X-Y) images and 3D reconstructions that provide an X-Z representation of the synapse as seen from the APC side. In contrast, control experiments involving T cells interacting with the membranes of antigen-free APC showed a homogenous pattern of moesin localization, including within the zone of cell-cell contact (Figure 1B).

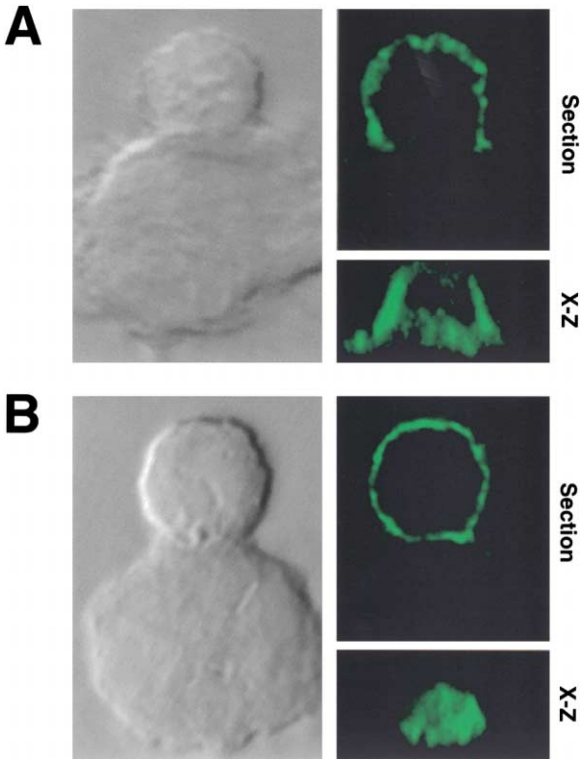

Figure 1. Intracellular Localization of Moesin in T Cells

Examples of moesin distribution in T cells interacting with an antigen-pulsed APC (A) or with an unpulsed APC (B). Each sample includes a gray scale DIC image showing the small T cell at the top contacting the larger APC along with two green fluorescent images, a cross-section view (top) and an X-Z reconstruction of the mature synapse as viewed from the perspective of the APC (bottom).

To address more precisely where moesin localizes compared to a previously characterized component of the synapse, two-color stainings were performed for moesin and talin. Our results show that these two members of the Band 4.1 protein superfamily expressed in T cells are spatially segregated in the mature synapse (Figure 2A). Moesin appears to overlap only slightly at the outermost edge of the talin ring previously shown to surround the zone of increased TCR density (Monks et al., 1998). This distribution represents a very broad region of exclusion and suggests that moesin collects outside of what could be considered the effective syn-

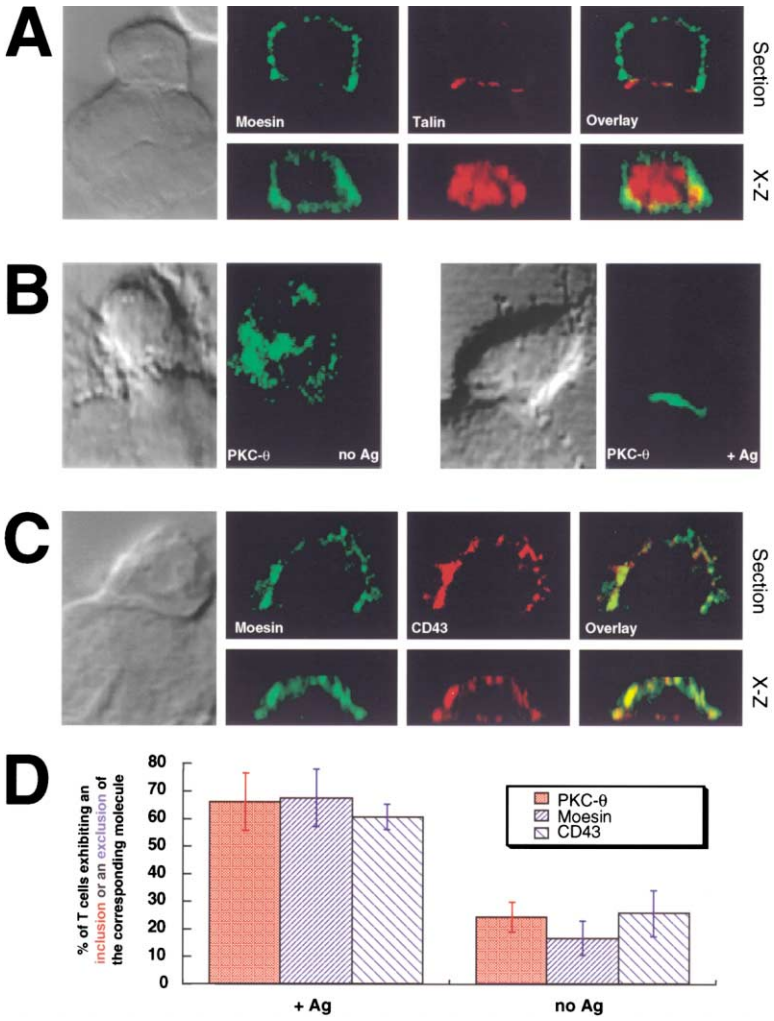

Figure 2. Relative Distribution of Moesin Compared to Other Molecules in the Mature Synapse

(A) Two-color staining for moesin (green) and talin (red) in a T cell engaged in an antigen-specific conjugate.

(B) One-color staining for PKC-θ in a T cell engaged in an unspecific (left) or antigen-specific (right) conjugate. Concentration of PKC-θ in the synapse is clearly observed in the presence of antigen.

(C) Two-color staining of moesin (green) and CD43 (red) in a T cell engaged in an antigen-specific conjugate. Both proteins are coexcluded from the region of close cell-cell membrane contact.

(D) Percentage of T cells with PKC-θ inclusion in the T-APC contact region or with moesin and CD43 exclusion from this region in the presence (left) or absence (right) of antigen. Bars represent mean ± SE for at least three independent experiments. A total of 303 blindly imaged T-APC conjugates were included in this analysis.

apse, defined by the tight adhesive ring formed by the integrin LFA-1 and its underlying talin partner.

Because of the reported association of moesin and CD43, we examined if the described exclusion of CD43 from the synapse (Sperling et al., 1998) actually paralleled this very broad exclusion of moesin. The localization of moesin and CD43 was analyzed in parallel using T cells interacting with antigen-bearing or antigen-free APC. The position of the central synapse was determined by staining for PKC-θ (Figure 2B). Two-color staining showed colocalization of CD43 and moesin in these cells (Figure 2C). Examination of the contact zone using X-Z projections revealed the exclusion of moesin and CD43 to be essentially complete, with no evidence of substantial numbers of small clusters remaining, in contrast to what has been reported for CD45 (Johnson et al., 2000). These findings reveal the parallel exclusion of moesin and CD43 from the synapse and also extend the spatial resolution of an earlier report describing just the cross-sectional pattern of CD43 distribution in the region of T-APC contact (Sperling et al., 1998). Under the same conditions, CD44 was not coexcluded with moesin (data not shown). Both moesin and CD43 were found to be absent from the region marked by PKC-θ in at least 70% of the antigen-specific conjugates (Figure 2D).

Moesin Is Dephosphorylated upon Antigen Recognition

The colocalization of CD43 and moesin described above is consistent with previous data showing that these molecules can bind to one another (Serrador et al., 1998; Yonemura et al., 1998). This raised the possibility that changes in CD43 localization upon TCR engagement might be due to a primary effect of TCR signaling on moesin distribution. Current models of ERM protein function postulate a key role for phosphorylation in regulating the interaction of these proteins with both transmembrane molecules and the actin cytoskeleton. We therefore examined whether TCR signaling affected moesin threonine phosphorylation. For this purpose, we made use of an antibody that recognizes specifically the T558 phosphorylated form of this molecule (Oshiro et al., 1998) and analyzed by Western blot the pattern of moesin phosphorylation in T cells activated by peptide-pulsed or unpulsed APCs (Figures 3A and 3B). T lymphocytes alone or in contact with the control antigen-free APCs have a high level of moesin phosphorylation. Anti-

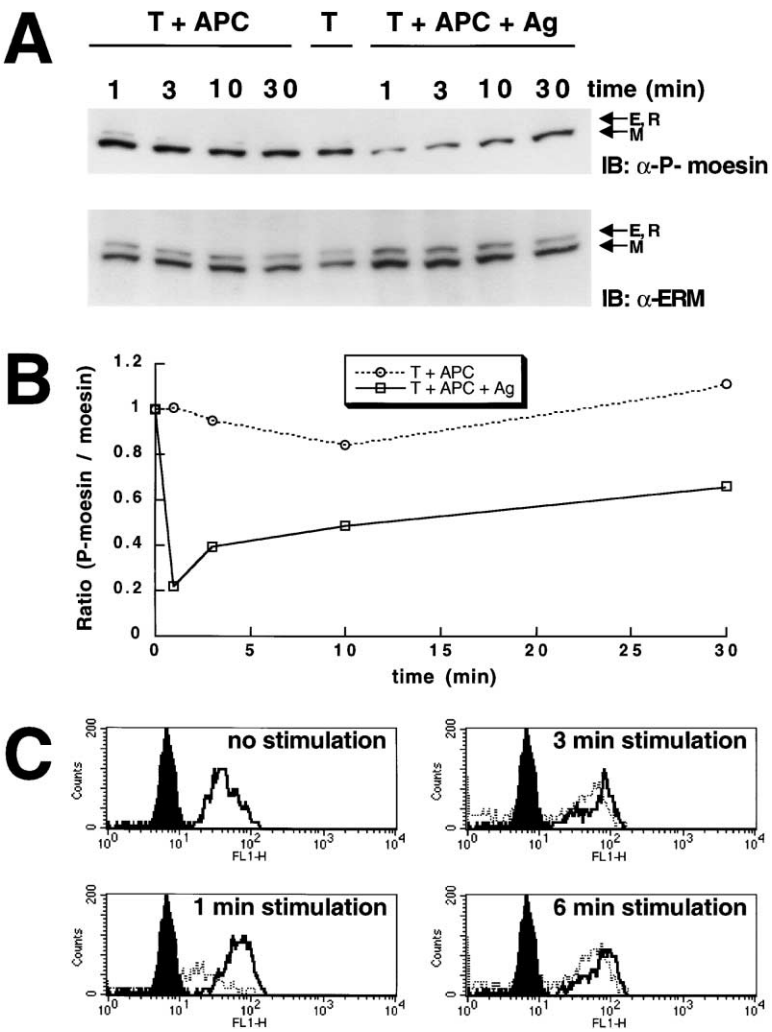

Figure 3. Biochemical Analysis of Moesin T558 Phosphorylation in T Cells

(A) T cells alone (T) and T cells interacting with unpulsed (T + APC) or antigen-pulsed (T + APC + Ag) APC were lysed after different times of contact as indicated, and the phospho-moesin content (top) versus total ERM level (bottom) was analyzed by Western blot.

(B) Densitometric quantitation of the relevant bands in the gel presented in (A). For the different conditions, the intensities of the bands were measured as described in Experimental Procedures, and the ratio (P-moesin/moesin) was calculated.

(C) Phospho-moesin content of T cells stimulated by soluble anti-CD3 antibody. Unstimulated T cells (no stimulation) were stained with an irrelevant rabbit IgG (black histogram) or anti-pT558 (thick line). T cells stimulated with an irrelevant hamster IgG (thick line) or with anti-CD3 antibody (dotted line) for different periods of time (1–6 min stimulation) were stained with anti-pT558. The negative control of the staining is superimposed as a black histogram.

gen recognition triggers rapid (<1 min) moesin dephosphorylation. Threonine phosphorylation of moesin is then partially regained over the next few minutes. We were also able to elicit moesin dephosphorylation by anti-CD3 antibody stimulation alone (Figure 3C), suggesting that TCR signaling in the absence of integrin or CD28-dependent costimulation is sufficient to trigger this effect.

In order to correlate at the single-cell level these changes in moesin phosphorylation with the physical position of other markers, four-color immunocytochemical staining for moesin, phospho-moesin, CD43, and TCR was performed on cells fixed at various times following initiation of T-APC contact (Figure 4). Consistent with the biochemistry experiments previously described, T cells interacting with unpulsed APCs showed a strong staining for phospho-moesin. TCRs, moesin, and CD43 remained largely homogenously distributed in these T cells. In contrast, after 1 min of interaction with peptide-pulsed APCs the level of phospho-moesin staining in T cells was nearly at background levels, not just in the contact region but throughout the entire cell. At this very early time, we could also detect the first signs of CD43 exclusion in the X-Z view as a relative depletion in this protein in the center of the interface as compared to the periphery of the contact region. However, at this time point, the TCR distribution was still grossly unchanged. By 3 min, an increase in T558 phosphorylated moesin molecules was only seen in the synapse but not in the very center where TCR molecules started to accumulate. As time progressed, the phosphorylation levels of moesin continued to rise and included the bulk of the molecules outside the synapse. The coexclusion of the phospho-moesin/CD43 complexes from the contact zone became more pronounced as this rephosphorylation proceeded over the next 5–10 min, generating an extensive region devoid of these molecules and at the same time, enriched in TCRs. This area tended to enlarge with time until reaching the pattern seen in the mature synapse stage (Figure 1).

Only Phospho-Moesin Is Able to Bind CD43

Because antigen-specific signals result in the dephosphorylation of moesin at T558, we next examined whether the phosphorylation state of moesin molecules affected interaction with CD43. We coexpressed a CD43-GFP chimeric protein in 293T cells along with HA-tagged moesin molecules containing either the T558A mutation that yields a molecule acting like dephosphorylated moesin or a T558D mutation that produces a pro-

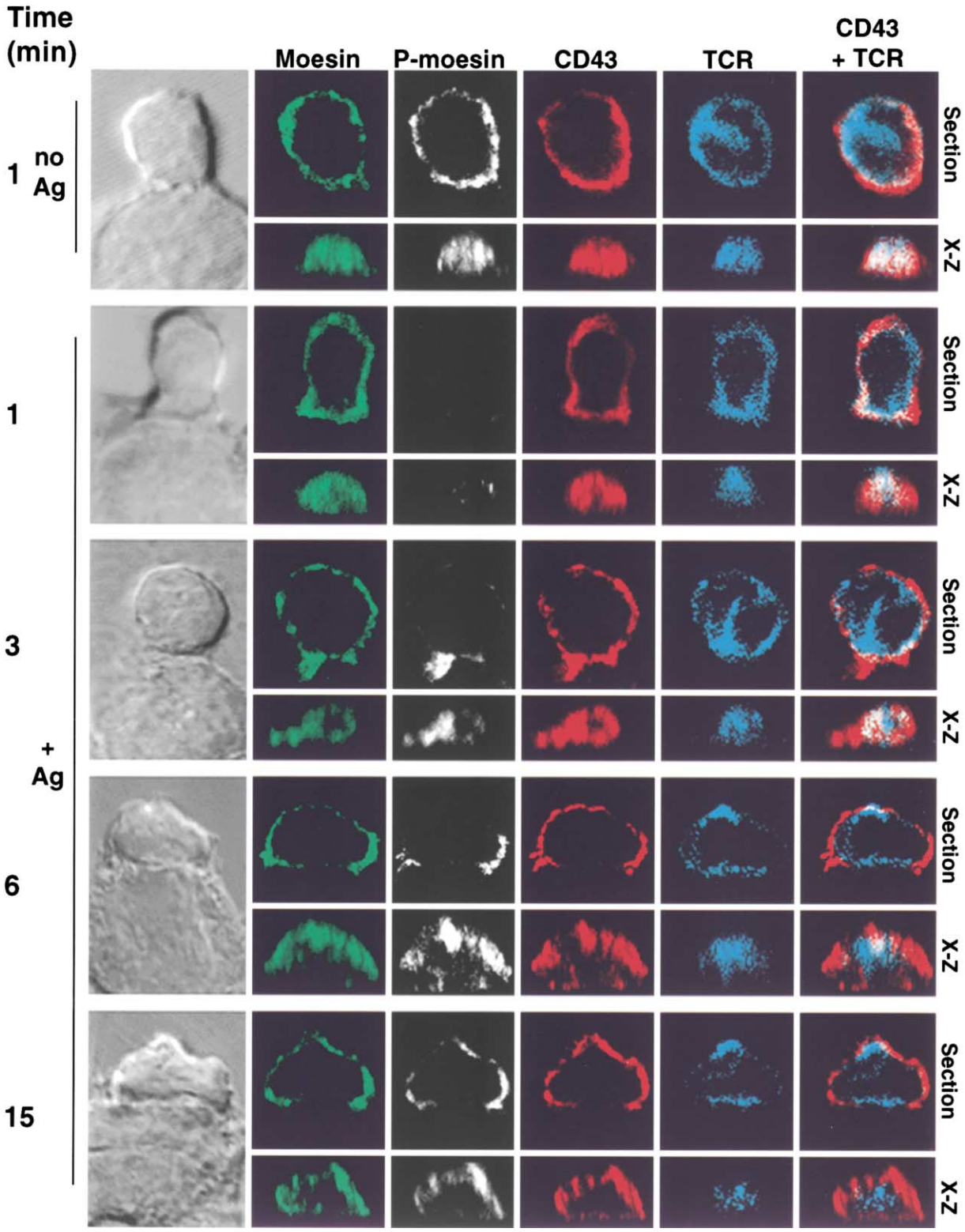

Figure 4. Kinetics of Redistribution of Moesin, Phospho-Moesin, CD43, and TCR Following Exposure to APC

Four-color staining for moesin (green), phospho-moesin (white), CD43 (red), and TCR (blue) was performed on T cells interacting for the times indicated with unpulsed APC (top panel) or antigen-pulsed APC (bottom four panels). CD43 and TCR stainings were also superimposed (right column). Regions corresponding to TCR-CD43 colocalization appear in white.

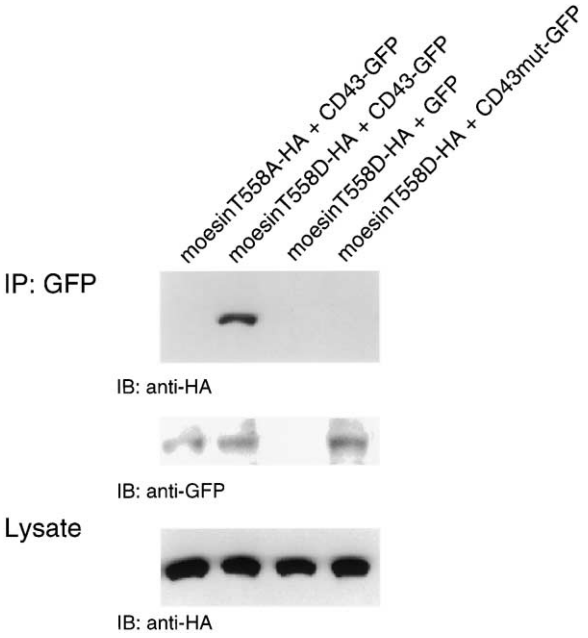

Figure 5. Biochemical Analysis of the Association between Moesin and CD43

293T cells were cotransfected with pairs of plasmids encoding moesin and either GFP, CD43-GFP, or CD43mut-GFP. GFP-containing proteins were immunoprecipitated (IP), and blots were probed with an anti-HA antibody (top) and an anti-GFP antibody (middle; note: GFP runs too far below the CD43-GFP chimeras to be visualized in this condition, but other experiments confirmed comparable expression of the free GFP under these conditions). The whole-cell lysate was probed with the anti-HA antibody (bottom) to establish that a similar level of moesin was expressed in the different conditions.

tein mimicking the phosphorylated form of this adaptor (Oshiro et al., 1998; Huang et al., 1999). Association between these mutant moesin molecules and the coexpressed CD43-GFP was assessed by immunoprecipitation. Figure 5 shows that only the moesinT558D mutant was able to bind to CD43. Together with a previous report suggesting that this particular mutant is the only one able to bind actin filaments (Huang et al., 1999), these results indicate that moesin phosphorylation on T558 is crucial for the molecule to play its role as a crosslinker between the cortical actin cytoskeleton and CD43.

A CD43 Mutant Protein that Cannot Bind Phospho-Moesin Fails to Remain Stably Excluded from the Synapse

The combination of moesin-CD43 colocalization experiments and these association studies suggested a relationship between the interaction of these molecules and their TCR-regulated redistribution in antigen-stimulated T cells. To address this issue more directly, we took advantage of the fact that a recent report had shown that a cluster of positively charged amino acids in the juxtamembrane region of the cytoplasmic tail of rat CD43 is important for its binding to moesin (Yonemura et al., 1998). MoesinT558D was coexpressed in 293T cells together with CD43-GFP whose cytoplasmic tail had been mutated in these positive residues (referred to CD43mut-GFP). Immunoprecipitation experiments clearly showed a loss of association between the moesin and the mutant CD43 chimera (Figure 5), indicating that the mutation introduced in the cytoplasmic tail of CD43 interfered with moesin binding.

We next transduced activated 5C.C7 T cells with retroviruses encoding GFP alone, CD43-GFP, or CD43mut-GFP. These cells were then put together with antigen-pulsed APCs for 30 min, and the subcellular distribution of GFP fluorescence in live T cells engaged in conjugates was analyzed in each condition (Figure 6A). GFP alone gave the expected pattern of intracellular staining. In contrast, the GFP fusion proteins were mainly located at the plasma membrane. CD43-GFP was excluded from synapses at 30 min, as found previously for endogenous CD43 (Figure 6B). However, T lymphocytes expressing the CD43mut-GFP form failed to exclude these chimeric molecules and showed either a homogenous distribution or even an accumulation of CD43mut-GFP near the region of cell contact in the majority of cells. Thus, these data provide further support for the hypothesis that the association of CD43 with moesin is necessary for the positioning of CD43 in the periphery of the synapse.

A more complete spatio-temporal view of CD43 exclusion following T cell activation was achieved by producing high-resolution 4D movies of retrovirally transduced T cells interacting with antigen-pulsed APC, using the general method described by Krummel et al. (2000). A typical acquisition sequence consisted of a z stack of ten GFP images followed by ratiometric measurement of the intracellular calcium (Ca^{2+}) concentration as an indicator of early T cell activation and collection of a transmitted-light image for visualizing the T-APC conjugate. Imaging of T cells expressing CD43-GFP (Figure 6C; see Supplemental Movie S1 at http://www.immunity.com/cgi/content/full/15/5/691/DC1) confirmed the rapid (about 1 min) exclusion of CD43 seen previously in static stainings (Figure 4). The onset of the Ca^{2+} response was very rapid upon contact with the APC (in the order of 10–20 s) and contemporaneous with the onset of CD43 exclusion. In contrast, T cells expressing the CD43mut-GFP (Figure 6C; see Supplemental Movie S2 at http://www.immunity.com/cgi/content/full/15/5/691/DC1), although showing an initial exclusion of the nonanchored CD43mut-GFP molecules, failed to stably exclude these chimeric proteins from the T-APC contact in ~80% of the cell pairs examined. This particular cell image shows an example of the accumulation of excess CD43mut-GFP in the contact zone several minutes after initial cell-cell contact.

Some studies have suggested that CD43 acts as an inhibitor of T cell activation, possibly because its large size and high negative charge (Cyster et al., 1991) might interfere with close binding of the T cell and APC membrane (Manjunath et al., 1995). Because T cells expressing CD43mut-GFP fail to stably relocate this protein outside of the synaptic region within which the primary TCR recognition events are taking place, we hypothesized that these cells would exhibit a defect in T cell activation. This possibility was examined by using intracellular staining and flow cytometry to measure the IL-2 production of retrovirally transduced T cells expressing either GFP alone, the wild-type CD43-GFP chimera, or

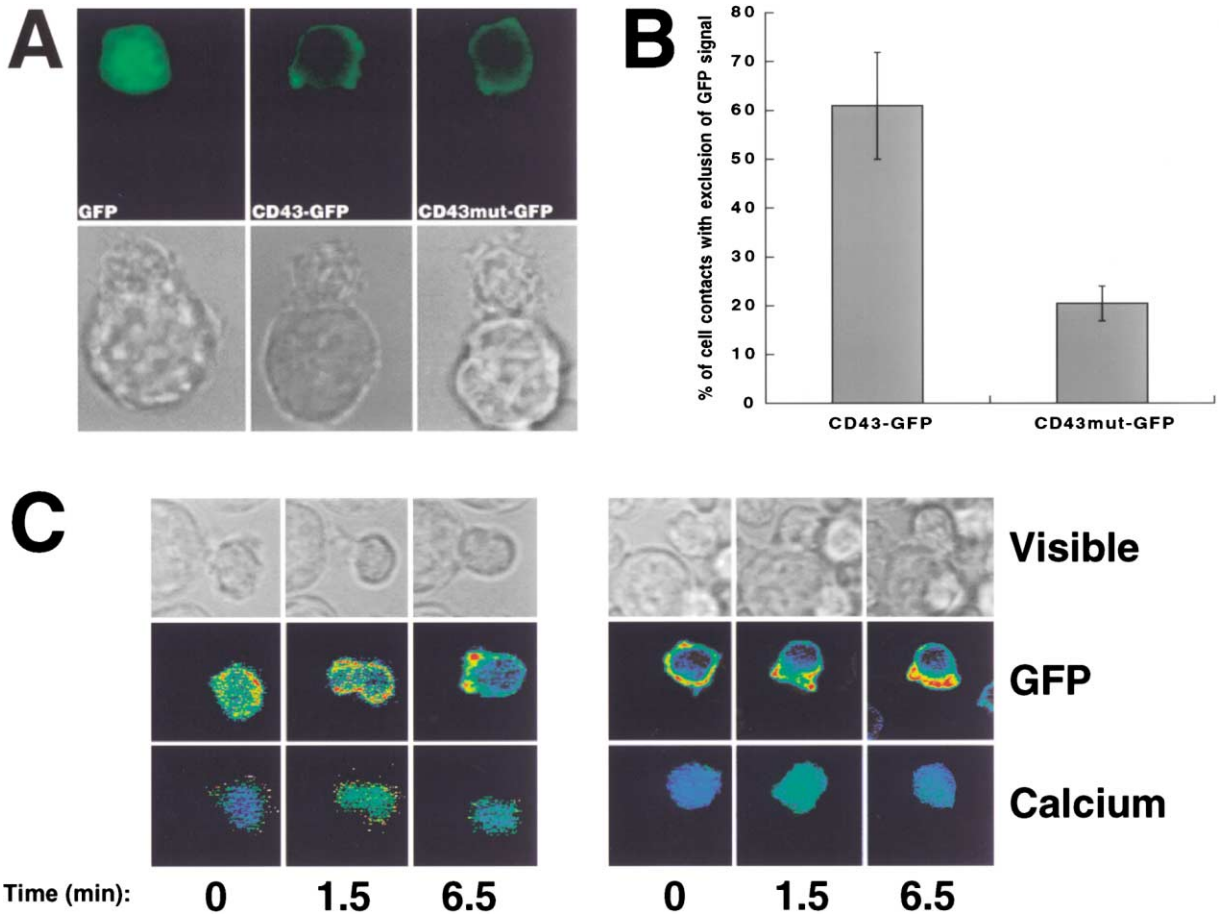

Figure 6. Subcellular Distribution of CD43-GFP Chimeric Proteins in Retrovirally Transduced T Cells Interacting with Pulsed APCs

(A) T cells expressing GFP (left), CD43-GFP (middle), or CD43mut-GFP (right) proteins were incubated in the presence of pulsed APCs and imaged after 30 min of contact.

(B) Percentage of T cells showing exclusion of the GFP signal from the synapse. Mean ± SE. A total of 49 cells were included in this analysis.

(C) Still images from video analysis of CD43-GFP$^+$ cells (left panel) and CD43mut-GFP$^+$ cells (right panel) interacting with antigen-bearing APC. Each series of images represents a transmitted-light image of the small T cell interacting with the larger APC (top), a fluorescent image for GFP (middle), and a Ca^{2+} ratio image (bottom) taken at 0, 1.5, and 6.5 min of cell contact. The Ca^{2+} and GFP images were pseudocolored using an arbitrary LUT with red representing the highest signal and blue the lowest; the range was 2 for GFP and 10 for Ca^{2+}.

the moesin nonbinding mutant form of this fusion protein (Figure 7). For all conditions, there was about a 40% reduction in the percentage of IL-2$^+$ cells among the infected cells with the highest CD43mut-GFP expression as compared to cells with equivalent expression of wild-type CD43-GFP.

Discussion

Considered together, the results presented here suggest the following thaw-freeze model of CD43 exclusion from the developing immunological synapse. Unstimulated T cells exhibiting a high level of moesin phosphorylation have cell-surface CD43 molecules anchored to the underlying cortical cytoskeleton via this ERM family adaptor. Very early TCR signals result in dephosphorylation of moesin that releases CD43 from the cytoskeleton, which we visualize as a loss of strict colocalization of CD43 and moesin at 1 min after cell contact. Such uncoupling of CD43 presumably increases the mobility of these molecules in the lipid bilayer. This may permit their rapid exclusion from the immediate vicinity of the accumulating TCR within the first minute of T-APC interaction, possibly by a passive mechanism based on molecular dimensions (Davis and van der Merwe, 1996; Shaw and Dustin, 1997) and membrane deformation (Qi et al., 2001). However, it is important to note that this freedom of movement only follows initiation of active ligand-induced TCR signaling that occurs in the presence of CD43 molecules initially intermingled with the resting distribution of TCR. The moesin rephosphorylation that follows this initial disanchoring event results in the rapid reattachment of CD43 molecules to the actin cytoskeleton in a zone that is only excluded from the most central portion of the synapse. Further movement of the CD43 to a peripheral location outside the LFA-1 ring appears to require this reanchoring, because mutant CD43 molecules unable to make this association fail to be more than initially excluded from the core of the synapse. At the mature stage of synapse formation,

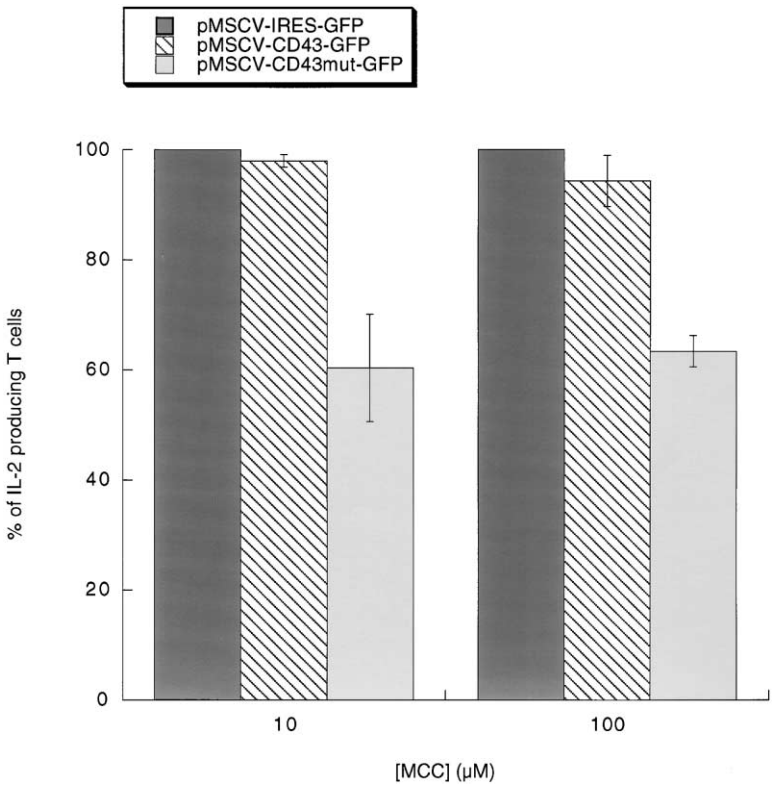

Figure 7. Production of IL-2 by T Cells Expressing Excess Wild-Type or Mutant CD43-GFP Proteins

T cells retrovirally transduced with pMSCV-IRES-GFP, pMSCV-CD43-GFP, or pMSCV-CD43mut-GFP vectors were incubated in presence of APCs prepulsed with different concentrations of antigen. Data are presented as the percentage of IL-2$^+$ T cells in the population (mean ± SE). The differences between CD43-GFP$^+$ and CD43mut-GFP$^+$ cells are statistically significant ($p < 0.02$ and $p < 0.01$ for 10 μM and 100 μM, respectively).

phospho-moesin molecules presumably facilitate stable T-APC adhesion by anchoring CD43 molecules well away from the active contact zone.

The dephosphorylation of moesin described here may represent a specific instance of a general modification of many cytoskeletal proteins, as it has been shown that Ser/Thr dephosphorylation of the cytoskeletal protein cofilin also occurs in T cells upon activation (Ambach et al., 2000). The global moesin dephosphorylation we observe may reflect what normally occurs upon T cell contact with an antigen-bearing APC or may be a consequence of the tight packing of T cells with numerous APC under the specific experimental conditions employed here to coordinately trigger a large population of T cells. In the former case, the disanchoring effect may be more local, affecting CD43 just in the vicinity of the forming synapse. The specific phosphatase(s) and kinase(s) responsible for regulating moesin phosphorylation in T lymphocytes, in particular those responding to signals arising from engagement of the TCR, remain unidentified. The phosphatases PP2C (Hishiya et al., 1999) and myosin phosphatase (Fukata et al., 1998), which have previously been reported to act on moesin, are possibilities for the effector enzymes activated by a TCR-induced messenger.

With respect to moesin rephosphorylation, several different kinases have been shown to act on ERM proteins. For example, Rho-kinase has been suggested to participate in cytoskeletal remodeling by phosphorylating this family of proteins (Fukata et al., 1998; Matsui et al., 1998; Oshiro et al., 1998). Interestingly, PKC-θ has also been shown to activate moesin by phosphorylating T558 (Pietromonaco et al., 1998). Given the unique behavior of this kinase in activated T lymphocytes (Monks et al., 1997), this PKC isoform represents another attractive candidate for TCR-dependent regulation of moesin activity. Experiments with gene-targeted cells, cells expressing dominant-negative forms of these candidate phosphatases or kinases, or cells whose expression of these proteins is reduced using antisense approaches will be necessary to determine if these or other enzymes are involved in the sequential change of moesin phosphorylation seen following TCR engagement.

The exact role of CD43 in TCR-mediated lymphocyte activation is still debated in the literature, with some reports suggesting an inhibitory role (Manjunath et al., 1995), others an activating/costimulatory function (Park et al., 1991; Sperling et al., 1995), and still others no role at all (Carlow et al., 2001). Our studies with the CD43mut-GFP molecule are consistent with this protein playing a negative role during cell-cell interactions. The inhibitory effect on cytokine responses seen when this large, highly charged molecule is prevented from leaving the synapse is consistent with a previous report showing inhibition of T cell activation in cells expressing an elongated CD48 molecule (Wild et al., 1999). In this latter case, the additional distance between T cell and APC membrane resulting from the modified length of the CD48-CD2 pair is presumed to limit effective TCR-ligand interaction, and a similar effect could be imagined when CD43 remains interspersed with TCR in the maturing synapse. Alternatively, the firm adhesion necessary for prolonged cell-cell contact might be compromised in both of these cases, leading to premature cessation in the signals necessary for gene activation (Iezzi et al., 1998). This latter possibility is more in accord with our

failure to see obvious changes in early TCR-associated phosphorylation in cells expressing CD43mut-GFP (our unpublished observations).

In some instances, it has been possible to visualize clusters of CD43 molecules in the synapse 1–3 min after the T-APC contact, when some moesin and CD43 molecules are still present in this zone. Within the next few minutes, larger-scale movement of molecules seems to occur, with CD43 stably maintained outside the synapse by its moesin anchoring. This sequence of initial small-scale segregation followed by partitioning of distinct proteins in different regions of the membrane, first proposed to occur at a submicroscopic scale by van der Merwe et al. (2000) in considering how TCR signaling is initiated, is consistent with the experimental results reported here.

T cells can achieve a high degree of prepolarization when stimulated by chemokines (Serrador et al., 1998). This is typically visualized as a change in the overall morphology of the T cell, which loses its typical round shape and adopts a more elongated one with a leading edge and a uropod within which CD43 is concentrated. In the experiments described in the present paper, we did not observe any prepolarization of the rested T cells before contacting the APC (for example, see Supplemental Movie S1 at http://www.immunity.com/cgi/content/full/15/5/691/DC1). Cells had a round shape with a relatively homogenous distribution of CD43. Thus, it is clear that our APCs did not induce any T cell polarization phenomena mediated by soluble molecules. It is unknown whether in more physiological in vivo conditions a T cell present in the lymph node would show prepolarization of surface proteins such as CD43 before contacting an APC. In situ tracking of T-APC conjugate formation will be necessary to address this question.

Two final points relate to the architecture of the plasma membrane in the mature T-APC contact zone and to the physiological relevance of moesin exclusion upon antigen recognition. Moesin phosphorylated at T558 shows a preferential distribution to microvilli in various cell types (Oshiro et al., 1998; Yonemura and Tsukita, 1999), and ERM antisense oligonucleotides expressed in thymoma cells causes the cells to lose their microvilli and adopt a "bald" state (Takeuchi et al., 1994). We confirmed the localization of moesin in microvilli in this study (within the limits of light microscopy) based on z sections encompassing the cell surfaces of T cells engaged in a conjugate (data not shown). Therefore, it is tempting to speculate that the initial moesin dephosphorylation upon antigen recognition leads to the breakdown of microvilli and a flattened surface membrane on the T cell that could favor (short) lymphocyte surface proteins binding to their respective ligands on the APC. This topographic change would be maintained over time by the exclusion of rephosphorylated moesin from the synapse.

Lastly, because moesin is often considered as a marker for the cortical actin cytoskeleton, the particular pattern of moesin distribution described here would suggest that this actin network is largely excluded from the synapse. Those actin filaments that are present in the synapse might instead come from a newly polymerized pool generated in response to antigen recognition. These filaments may be responsible for generating the dynamic membrane protrusions that characterize the T-APC contact and that one can easily observe in video images of T-APC conjugates (see Supplemental Movies S1 and S2 at http://www.immunity.com/cgi/content/full/15/5/691/DC1). Furthermore, polarization of microtubules toward the synapse is believed to play a role in directing the trafficking of secretory vesicles to the region of cell contact. Treatment of cells with the Ser/Thr phosphatase inhibitor calyculin A increases the F-actin association at the plasma membrane presumably by increasing ERM phosphorylation (Patterson et al., 1999), interfering with secretion-related processes. Thus, it would also be useful for the T cell to have a zone devoid of moesin so that the cortical actin microfilaments would not act as a barrier for the fusion of intracellular vesicles with the plasma membrane. This would suggest that the immunological synapse would be the ideal place for such secretory phenomena to take place, and this idea fits quite well with one of the major *raison d'être* of the synapse: the polarized secretion of lymphocyte proteins toward the APC.

Experimental Procedures

Constructs

MoesinT558A and moesinT558D plasmid expression constructs (Oshiro et al., 1998) were each modified using PCR to contain a HA-coding sequence at the 3′ end of the original coding region. Inserts were then subcloned into the pcDNA3.1$^+$ vector (Invitrogen, Carlsbad, CA).

A fragment encoding murine CD43 plus a linker (amino acid composition: GGGGGGGGGA) was amplified from the pBabe-CD43 plasmid (a gift from Dr. J. Green, Washington University, St. Louis, MO) and subcloned into the MSCV-IRES-GFP retroviral vector (Van Parijs et al., 1999) in place of the IRES cassette but in frame with GFP. Site-directed mutagenesis of CD43 to mutate residues 276–278 from KRR to NGG was conducted using the QuickChange kit (Stratagene, La Jolla, CA) and the appropriate primers.

Transfection/Retroviral Infection

Transient transfections of the human kidney 293T cell line were performed using FuGENE 6 (Roche, Indianapolis, IN) according to manufacturer's instructions.

Supernatants from Phoenix cells stably producing retroviruses encoding GFP, CD43-GFP, or CD43mut-GFP were filtered through 0.45 μm membranes, then supplemented with 10 μg/ml polybrene (Sigma, St. Louis, MO) and 1 ng/ml IL-2 (BD Pharmingen, San Diego, CA). They were added to recently antigen-stimulated 5C.C7 TCR transgenic × RAG-2$^{-/-}$ T cells and spun at 2,600 rpm for 90 min at 26°C. Typically, retroviral transduction of one cell culture involved a total of five rounds of such spin infection on days 1 to 3 after stimulation.

Microscopy

Primed 5C.C7 T lymphocytes were mixed together with 10–100 μM MCC (88–103) antigenic peptide-pulsed LK35.2 B cell lymphoma and allowed to interact on poly-lysine precoated glass coverslips. After different times of contact, cells were fixed with 4% paraformaldehyde for 10 min, permeabilized with 0.1% Triton X-100 for 10 min, and stained for 45 min with the following antibodies: anti-moesin (Santa Cruz Biotechnology, Inc., Santa Cruz, CA), anti-talin (clone 8d4; Sigma), anti-CD43 (clone S7; BD Pharmingen), anti-PKC-θ (Santa Cruz), biotinylated anti-TCRβ (clone H57; BD Pharmingen), and/or anti-pT558 (Oshiro et al., 1998). Primary antibodies were revealed using donkey-anti-species secondary antibodies conjugated to FITC, Texas red, or Cy5 and streptavidin-AMCA (Jackson ImmunoResearch, West Grove, PA). Stained cells were visualized with a Leica TCS-NT/SP confocal microscope (Leica Microsystems) using a 100× oil immersion objective (NA 1.4). Forty to fifty z sections separated by 0.2 μm were acquired. Rotations and X-Z reconstruc-

tions of images were performed using the Autoaligner and Imaris software systems from BitPlane (Zürich, Switzerland).

Experiments involving live cell imaging of retrovirally transduced T lymphocytes were performed at 37°C on a conventional epifluorescence DMIRBE Leica microscope. Images were acquired using a 63× oil immersion objective and a Hamamatsu Orca 2 digital camera (C4742-98) (Hamamatsu Photonics K.K., Sunayama-Cho, Japan). Storage, processing, and deconvolution were done using OpenLab software from Improvision (Coventry, England). A sequence of acquisition (one complete sequence every 30 s) comprised the rapid capture of a z stack of GFP pictures (typically 10 sections of 1 μm step in ~5 s using the "critical session" option of the software), a ratio measurement of Fura-2 fluorescence for the assessment of intracellular calcium levels, and a transmitted-light image.

Intracellular Staining for Flow Cytometry

To quantitate the number of cells producing IL-2 upon antigen stimulation, T cells were stimulated as described below, fixed, permeabilized, stained with PE-conjugated anti-mouse IL-2 antibody (BD Pharmingen), and analyzed using a FACScan flow cytometer (Becton Dickinson, San Jose, CA).

For analysis of phospho-moesin content, unstimulated T cells or T cells stimulated with 20 μg/ml of soluble anti-CD3-ε antibody (2C11; BD Pharmingen) or hamster IgG (BD Pharmingen) were stained with a rabbit IgG or with anti-pT558. Primary antibodies were revealed using FITC-conjugated anti-rabbit antibodies (Jackson ImmunoResearch).

Biochemistry

For anti-pT558 immunoblots, T cells were spun together with APCs at 1,000 rpm for 10 s and allowed to interact for various periods of time at 37°C. The pellets were then resuspended in cold RIPA buffer (0.1% sodium dodecyl sulfate [SDS], 0.5% deoxycholate, 1% Nonidet P-40 [Pierce, Rockford, IL], 150 mM NaCl, 50 mM Tris-HCl [pH 8], complete proteases inhibitors cocktail [Roche], and phosphatase inhibitors) for 30 min and then centrifuged for 15 min at 14,000 rpm at 4°C. Pellets were discarded and the supernatants were resuspended in SDS-sample buffer and boiled for 5 min at 95°C. Samples were loaded in a 10% Tris-Glycine gel. After migration, the proteins were transferred onto a PVDF membrane (Millipore, Bedford) by electroblotting. Proteins were revealed using the anti-pT558 antiserum and a goat anti-rabbit-HRP secondary reagent (BioRad) followed by ECL development. The membrane was then stripped according to manufacturer's protocol (Pierce) and reprobed with an anti-ERM antiserum (Santa Cruz) followed by anti-goat-HRP (BioRad) and chemiluminescence exposure.

Densitometry quantification was performed by scanning and analyzing X-ray films using a Kodak Image station 440CF and Kodak Digital Sciences 1D software. Density values for each blot were normalized by giving the arbitrary value of 1 to the band corresponding to unstimulated T cells.

For immunoprecipitation experiments, 293T cells transiently transfected 40 hr earlier were lysed in ice-cold lysis buffer (150 mM NaCl, 10 mM HEPES [pH 7.5], 0.1% NP-40, 1 mM DTT, 20 μg/ml leupeptin) for 30 min at 4°C. Lysates were centrifuged for 15 min at 14,000 rpm at 4°C. Pellets were discarded and the supernatants were resuspended in SDS-sample buffer and boiled (whole-cell lysate) or immunoprecipitated. The latter involved mixing 950 μl of lysate with 50 μl of protein-G^+ agarose (Santa Cruz) precoated with anti-GFP antibodies (Roche) and incubating the mixture for 2 hr with constant agitation. Beads were washed four times in lysis buffer, and pellets were resuspended in SDS-sample buffer, boiled, and subjected to electrophoresis in a 7.5% Tris-Glycine gel. The proteins were transferred to a PVDF membrane and revealed with anti-HA (Covance, Denver, CO) and anti-GFP primary antibodies, HRP-conjugated secondary reagents, and chemiluminescence.

IL-2 Production

Unsorted T cell infectants were added to LK35.2 cells prepulsed overnight with 10–100 μM MCC (88–103) peptide. After a 3–4 hr incubation period in the presence of 2 μM monensin, T cells were harvested and processed for intracellular staining. Results are presented as (% of $GFP^{bright}IL\text{-}2^+$ cells/% of $GFP^-IL\text{-}2^+$ cells) × 100. For each antigen concentration, the data were normalized to 100% for the control condition. Results from three independent experiments were pooled together.

Acknowledgments

We thank Drs. S. Tsukita, J. Green, and H. Ziltener for providing reagents in the course of this study; Dr. Owen Schwartz (NIAID confocal facility) for help in the acquisition of images; Drs. K. Eichelberg and G. Bonnet for helpful advice during the course of these experiments; and Drs. A. Trautmann and G. Bonnet for critical reading of the manuscript. This work was supported by long-term postdoctoral fellowships from the European Molecular Biology Organization and the Human Frontier Science Program (J.D.).

Received April 23, 2001; revised September 4, 2001.

References

Acuto, O., and Cantrell, D. (2000). T cell activation and the cytoskeleton. Annu. Rev. Immunol. *18*, 165–184.

Ambach, A., Saunus, J., Konstandin, M., Wesselborg, S., Meuer, S.C., and Samstag, Y. (2000). The serine phosphatases PP1 and PP2A associate with and activate the actin-binding protein cofilin in human T lymphocytes. Eur. J. Immunol. *30*, 3422–3431.

Bretscher, A., Chambers, D., Nguyen, R., and Reczek, D. (2000). ERM-Merlin and EBP50 protein families in plasma membrane organization and function. Annu. Rev. Cell Dev. Biol. *16*, 113–143.

Bromley, S.K., Burack, W.R., Johnson, K.G., Somersalo, K., Sims, T.N., Sumen, C., Davis, M.M., Shaw, A.S., Allen, P.M., and Dustin, M.L. (2001). The immunological synapse. Annu. Rev. Immunol. *19*, 375–396.

Carlow, D.A., Corbel, S.Y., and Ziltener, H.J. (2001). Absence of CD43 fails to alter T cell development and responsiveness. J. Immunol. *166*, 256–261.

Cyster, J.G., Shotton, D.M., and Williams, A.F. (1991). The dimensions of the T lymphocyte glycoprotein leukosialin and identification of linear protein epitopes that can be modified by glycosylation. EMBO J. *10*, 893–902.

Davis, S.J., and van der Merwe, P.A. (1996). The structure and ligand interactions of CD2: implications for T-cell function. Immunol. Today *17*, 177–187.

Delon, J., and Germain, R.N. (2000). Information transfer at the immunological synapse. Curr. Biol. *10*, R923–R933.

Delon, J., Bercovici, N., Liblau, R., and Trautmann, A. (1998a). Imaging antigen recognition by naive $CD4^+$ T cells: compulsory cytoskeletal alterations for the triggering of an intracellular calcium response. Eur. J. Immunol. *28*, 716–729.

Delon, J., Bercovici, N., Raposo, G., Liblau, R., and Trautmann, A. (1998b). Antigen-dependent and -independent Ca^{2+} responses triggered in T cells by dendritic cells compared with B cells. J. Exp. Med. *188*, 1473–1484.

del Pozo, M.A., Vicente-Manzanares, M., Tejedor, R., Serrador, J.M., and Sanchez-Madrid, F. (1999). Rho GTPases control migration and polarization of adhesion molecules and cytoskeletal ERM components in T lymphocytes. Eur. J. Immunol. *29*, 3609–3620.

Dustin, M.L., and Cooper, J.A. (2000). The immunological synapse and the actin cytoskeleton: molecular hardware for T cell signaling. Nat. Immunol. *1*, 23–29.

Dustin, M.L., Olszowy, M.W., Holdorf, A.D., Li, J., Bromley, S., Desai, N., Widder, P., Rosenberger, F., van der Merwe, P.A., Allen, P.M., and Shaw, A.S. (1998). A novel adaptor protein orchestrates receptor patterning and cytoskeletal polarity in T-cell contacts. Cell *94*, 667–677.

Fukata, Y., Kimura, K., Oshiro, N., Saya, H., Matsuura, Y., and Kaibuchi, K. (1998). Association of the myosin-binding subunit of myosin phosphatase and moesin: dual regulation of moesin phosphorylation by Rho-associated kinase and myosin phosphatase. J. Cell Biol. *141*, 409–418.

Grakoui, A., Bromley, S.K., Sumen, C., Davis, M.M., Shaw, A.S., Allen, P.M., and Dustin, M.L. (1999). The immunological synapse: a

molecular machine controlling T cell activation. Science *285*, 221–227.

Heiska, L., Alfthan, K., Gronholm, M., Vilja, P., Vaheri, A., and Carpen, O. (1998). Association of ezrin with intercellular adhesion molecule 1 and -2 (ICAM-1 and ICAM-2). Regulation by phosphatidylinositol *4*, 5-bisphosphate. J. Biol. Chem. *273*, 21893–21900.

Helander, T.S., Carpen, O., Turunen, O., Kovanen, P.E., Vaheri, A., and Timonen, T. (1996). ICAM-2 redistributed by ezrin as a target for killer cells. Nature *382*, 265–268.

Hishiya, A., Ohnishi, M., Tamura, S., and Nakamura, F. (1999). Protein phosphatase 2C inactivates F-actin binding of human platelet moesin. J. Biol. Chem. *274*, 26705–26712.

Huang, L., Wong, T.Y., Lin, R.C., and Furthmayr, H. (1999). Replacement of threonine *558*, a critical site of phosphorylation of moesin in vivo, with aspartate activates F-actin binding of moesin. Regulation by conformational change. J. Biol. Chem. *274*, 12803–12810.

Iezzi, G., Karjalainen, K., and Lanzavecchia, A. (1998). The duration of antigenic stimulation determines the fate of naive and effector T cells. Immunity *8*, 89–95.

Johnson, K.G., Bromley, S.K., Dustin, M.L., and Thomas, M.L. (2000). A supramolecular basis for CD45 tyrosine phosphatase regulation in sustained T cell activation. Proc. Natl. Acad. Sci. USA *97*, 10138–10143.

Krummel, M.F., Sjaastad, M.D., Wülfing, C., and Davis, M.M. (2000). Differential clustering of CD4 and CD3ζ during T cell recognition. Science *289*, 1349–1352.

Kupfer, A., Swain, S.L., and Singer, S.J. (1987). The specific direct interaction of helper T cells and antigen-presenting B cells. II. Reorientation of the microtubule organizing center and reorganization of the membrane-associated cytoskeleton inside the bound helper T cells. J. Exp. Med. *165*, 1565–1580.

Lanzavecchia, A., and Sallusto, F. (2000). From synapses to immunological memory: the role of sustained T cell stimulation. Curr. Opin. Immunol. *12*, 92–98.

Leupin, O., Zaru, R., Laroche, T., Muller, S., and Valitutti, S. (2000). Exclusion of CD45 from the T-cell receptor signaling area in antigen-stimulated T lymphocytes. Curr. Biol. *10*, 277–280.

Mangeat, P., Roy, C., and Martin, M. (1999). ERM proteins in cell adhesion and membrane dynamics. Trends Cell Biol. *9*, 187–192.

Manjunath, N., Correa, M., Ardman, M., and Ardman, B. (1995). Negative regulation of T-cell adhesion and activation by CD43. Nature *377*, 535–538.

Matsui, T., Maeda, M., Doi, Y., Yonemura, S., Amano, M., Kaibuchi, K., and Tsukita, S. (1998). Rho-kinase phosphorylates COOH-terminal threonines of ezrin/radixin/moesin (ERM) proteins and regulates their head-to-tail association. J. Cell Biol. *140*, 647–657.

Monks, C.R., Kupfer, H., Tamir, I., Barlow, A., and Kupfer, A. (1997). Selective modulation of protein kinase C-θ during T-cell activation. Nature *385*, 83–86.

Monks, C.R., Freiberg, B.A., Kupfer, H., Sciaky, N., and Kupfer, A. (1998). Three-dimensional segregation of supramolecular activation clusters in T cells. Nature *395*, 82–86.

Oshiro, N., Fukata, Y., and Kaibuchi, K. (1998). Phosphorylation of moesin by rho-associated kinase (Rho-kinase) plays a crucial role in the formation of microvilli-like structures. J. Biol. Chem. *273*, 34663–34666.

Park, J.K., Rosenstein, Y.J., Remold-O'Donnell, E., Bierer, B.E., Rosen, F.S., and Burakoff, S.J. (1991). Enhancement of T-cell activation by the CD43 molecule whose expression is defective in Wiskott-Aldrich syndrome. Nature *350*, 706–709.

Parlato, S., Giammarioli, A.M., Logozzi, M., Lozupone, F., Matarrese, P., Luciani, F., Falchi, M., Malorni, W., and Fais, S. (2000). CD95 (APO-1/Fas) linkage to the actin cytoskeleton through ezrin in human T lymphocytes: a novel regulatory mechanism of the CD95 apoptotic pathway. EMBO J. *19*, 5123–5134.

Patterson, R.L., van Rossum, D.B., and Gill, D.L. (1999). Store-operated Ca^{2+} entry: evidence for a secretion-like coupling model. Cell *98*, 487–499.

Pietromonaco, S.F., Simons, P.C., Altman, A., and Elias, L. (1998). Protein kinase C-θ phosphorylation of moesin in the actin-binding sequence. J. Biol. Chem. *273*, 7594–7603.

Poo, W.J., Conrad, L., and Janeway, C.A., Jr. (1988). Receptor-directed focusing of lymphokine release by helper T cells. Nature *332*, 378–380.

Qi, S.Y., Groves, J.T., and Chakraborty, A.K. (2001). Synaptic pattern formation during cellular recognition. Proc. Natl. Acad. Sci. USA *98*, 6548–6553.

Serrador, J.M., Alonso-Lebrero, J.L., del Pozo, M.A., Furthmayr, H., Schwartz-Albiez, R., Calvo, J., Lozano, F., and Sanchez-Madrid, F. (1997). Moesin interacts with the cytoplasmic region of intercellular adhesion molecule-3 and is redistributed to the uropod of T lymphocytes during cell polarization. J. Cell Biol. *138*, 1409–1423.

Serrador, J.M., Nieto, M., Alonso-Lebrero, J.L., del Pozo, M.A., Calvo, J., Furthmayr, H., Schwartz-Albiez, R., Lozano, F., Gonzalez-Amaro, R., Sanchez-Mateos, P., and Sanchez-Madrid, F. (1998). CD43 interacts with moesin and ezrin and regulates its redistribution to the uropods of T lymphocytes at the cell-cell contacts. Blood *91*, 4632–4644.

Shaw, A.S., and Dustin, M.L. (1997). Making the T cell receptor go the distance: a topological view of T cell activation. Immunity *6*, 361–369.

Shcherbina, A., Bretscher, A., Kenney, D.M., and Remold-O'Donnell, E. (1999). Moesin, the major ERM protein of lymphocytes and platelets, differs from ezrin in its insensitivity to calpain. FEBS Lett. *443*, 31–36.

Simons, P.C., Pietromonaco, S.F., Reczek, D., Bretscher, A., and Elias, L. (1998). C-terminal threonine phosphorylation activates ERM proteins to link the cell's cortical lipid bilayer to the cytoskeleton. Biochem. Biophys. Res. Commun. *253*, 561–565.

Sperling, A.I., Green, J.M., Mosley, R.L., Smith, P.L., DiPaolo, R.J., Klein, J.R., Bluestone, J.A., and Thompson, C.B. (1995). CD43 is a murine T cell costimulatory receptor that functions independently of CD28. J. Exp. Med. *182*, 139–146.

Sperling, A.I., Sedy, J.R., Manjunath, N., Kupfer, A., Ardman, B., and Burkhardt, J.K. (1998). TCR signaling induces selective exclusion of CD43 from the T cell- antigen-presenting cell contact site. J. Immunol. *161*, 6459–6462.

Takeuchi, K., Sato, N., Kasahara, H., Funayama, N., Nagafuchi, A., Yonemura, S., and Tsukita, S. (1994). Perturbation of cell adhesion and microvilli formation by antisense oligonucleotides to ERM family members. J. Cell Biol. *125*, 1371–1384.

Tsukita, S., and Yonemura, S. (1999). Cortical actin organization: lessons from ERM (ezrin/radixin/moesin) proteins. J. Biol. Chem. *274*, 34507–34510.

Tsukita, S., Oishi, K., Sato, N., Sagara, J., and Kawai, A. (1994). ERM family members as molecular linkers between the cell surface glycoprotein CD44 and actin-based cytoskeletons. J. Cell Biol. *126*, 391–401.

van der Merwe, P.A., Davis, S.J., Shaw, A.S., and Dustin, M.L. (2000). Cytoskeletal polarization and redistribution of cell-surface molecules during T cell antigen recognition. Semin. Immunol. *12*, 5–21.

Van Parijs, L., Refaeli, Y., Lord, J.D., Nelson, B.H., Abbas, A.K., and Baltimore, D. (1999). Uncoupling IL-2 signals that regulate T cell proliferation, survival, and Fas-mediated activation-induced cell death. Immunity *11*, 281–288.

Wild, M.K., Cambiaggi, A., Brown, M.H., Davies, E.A., Ohno, H., Saito, T., and van der Merwe, P.A. (1999). Dependence of T cell antigen recognition on the dimensions of an accessory receptor-ligand complex. J. Exp. Med. *190*, 31–41.

Wülfing, C., and Davis, M.M. (1998). A receptor/cytoskeletal movement triggered by costimulation during T cell activation. Science *282*, 2266–2269.

Yonemura, S., and Tsukita, S. (1999). Direct involvement of ezrin/radixin/moesin (ERM)-binding membrane proteins in the organization of microvilli in collaboration with activated ERM proteins. J. Cell Biol. *145*, 1497–1509.

Yonemura, S., Hirao, M., Doi, Y., Takahashi, N., Kondo, T., and Tsukita, S. (1998). Ezrin/radixin/moesin (ERM) proteins bind to a positively charged amino acid cluster in the juxta-membrane cytoplasmic domain of CD44, CD43, and ICAM-2. J. Cell Biol. *140*, 885–895.